The correlated motion of electron pairs in Auger process within a single particle approach in angular momentum theory.

Candidato:

Eleonora Aquilini

Relatore esterno:

Prof. Giovanni Stefani

Matricola:

264418

Relatore interno:

Prof. Andrea Bruno

Anno Accademico 2005-2006

Classification:

The keys words: *Three Bodies Problem*, *Auger Effect*,

The aim of this thesis is to analyze a specific aspect of the "three bodies problem", a very interesting topic of research for both mathematics and physics, because it still unsolved even if it seems a simple problem. An interesting example of the three body problem is the "Auger effect" is that triggered off by irradiating the neutral atom A with photons; it can be divided in two separate processes: in the first step, the atom absorbs a photon creating a positive ion A^+ with a hole and making free an electron which was previously bound e_p^-; in the second step the ion decays into a double charged ion A^{++} and an internal electron called "Auger" is emitted e_A^-. Once the energy of the photon is set, the experiment consists in measuring, the energy and the quantity of motion of the final electrons. This approach is called "Two steps method". The scheme of the Auger effect that we want to study is represented in the fig 1, where
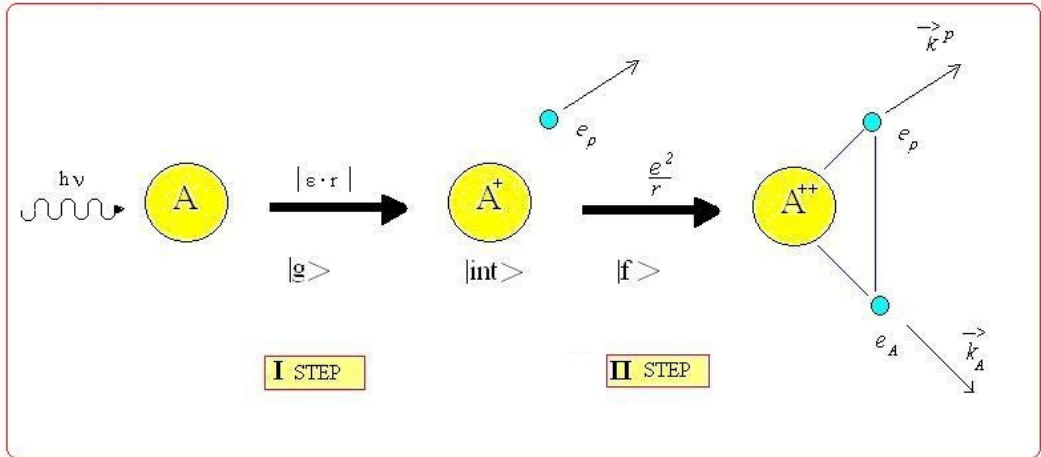
Figure 1: *: Example of the three bodies problem: Auger Effect*

$|g\rangle$ indicates the starting phase, $|int\rangle$ indicates the intermediate state between the two steps, and $\langle f|$ indicates the final state. In the formal manner we can write this process as

$$
\begin{aligned}
h\nu + A \quad &\rightarrow \quad A^+ + e_p^- \\
&\hookrightarrow \quad A^{++} + e_p^- + e_A^-
\end{aligned}
\tag{1}
$$

In order to analyze this process we consider a reference system which is centered on the

atom A; let's consider the triplet x, y, z where the axis z coincides with the direction of the propagation of the photons beam; the angles θ and ϕ are defined in the same way of a polar coordinates system. In our case we consider the light linearly polarized with polarization parallel to z axis.

In order to analyze this process, the formula which expresses the cross section must contain both the angular aspect of Schroedinger equation and also the radial matrix elements that regulate the process, which contain the radial wave functions involved in the transition. While in the first step a dipole approximation is used, in the second step the interaction reduces to a central Coulombian field.

The study has been made exclusively about a "closed shell" atom because in this way we can study this process like a "two bodies problem" and always applying "single particle" approximation where the effects on the wave functions caused by the presence of other electrons than those strictly involved in the transition are not considered. This approach leads to remarkably faster calculations than those implemented in literature, where a "multi-electron method" is used, which is a very powerful but time-consuming approach, that turns out to be impractical, if not inapplicable, to aggregates such as solids and molecules.

The targets of this thesis are:

1. To introduce the tools necessary to describe the cross section of the Auger process.

2. To study the Auger process focusing on the differential cross section, which is calculated fixing energy and momentum of one electron and varying the ejection angle of the other one. Calculations have been made on Xenon, at first disregard the effect of the radial elements, and then including them to observe how the symmetry of the cross section changes in the different kinetic condition.

3. To compare the experimental and "multi-electron" theoretical data present in literature [3], [4] with our single particle approach predictions.

4. To extend the study performed on Xe to Mg, which is a much lighter atom. In this way we can make some consideration about relevance of many electron effects

3

to the model which has been used and highlight relativistic and many-particles effects in the cross-section.

In the first chapter, it has been illustrated an introduction to quantum description of an atom, focusing on Schroedinger equation in the Hydrogen atom. Solving the Schroedinger equation for this very simply central field problem we can separate the radial variables from angular ones. This process is much important because it permits to study the angular dependence of the cross section independently from the radial matrix elements effects. This study is necessary to set the basis of knowledge needed in the order to understand the Auger effect.

In the second chapter we describe the collisions between electrons in order to be able to understand the nature of the collision which occurs within the Auger process that, as previously specified, is a Coulomb interaction.

In the third chapter we introduce the reader to angular momentum theory, which plays an important role in describing the Auger process, since it allows to cope with the angular momentum correlation which arise between the quantum numbers which characterize the electrons involved in the Auger transition.

In the last chapter, the core of this thesis, the Auger effect is studied under well defined initial conditions. By using the "method of the variables separation", we wanted firstly to understand the importance of the radial matrix elements in such a process. Secondly we have compared our results with the data obtained through the calculations available in literature to be able to understand value and limitation of the model that has been developed. As far the study of the emission of the two correlated electrons is concerned, the energy and angle differential cross section has been successfully calculated in the case of closed shell atoms like Xenon and Magnesium.

In the first appendix we write the Auger cross section calculus. In the other appendixes we write the calculation of the cross section of Xenon and Magnesium developed using Mathematica, including and excluding the radial matrix elements.

In calculate the transition probability we have need of different means: we indicate from $|g\rangle$ the initial state, $\langle f|$ the finish state, and $|int\rangle$ the intermediate state. The

calculations of the transition probability of the Auger effect, becomes easier if we adopt the central field model. Moreover, instead of considering all the electrons in the atom, we consider only the electrons strictly involved the transition, i.e we adopt a single particle approach.

Neglecting the relativistic effects, the interaction between the two electrons can be expressed approximately as follow [1]:

$$\frac{d^2\sigma}{dh_a dh_p} \propto \left| \left\langle \left| f \frac{e^2}{|\bar{r}_1 - \bar{r}_2|} \right| int \right\rangle \langle int \left| \bar{\epsilon} \cdot \bar{r} \right| g \rangle \right|^2$$

where $h_a = (\theta_a, \phi_a)$ and $h_p = (\theta_p, \phi_p)$, $|\bar{\epsilon} \cdot \bar{r}|$ indicates the dipole operator and $\frac{e^2}{|\bar{r}_1 - \bar{r}_2|}$ Coulomb one.

In the presence of a central field, a bound state can be written as [1]

$$|g\rangle = \sum_{n_c \sigma_c} \Re_{nl_c}(r) Y_{n_c l_c}(\hat{r}) X_{\sigma_c}$$

where X_{σ_c} represents the electron spin state, while the dipole operator $|\bar{\epsilon} \cdot \bar{r}|$ is a scalar product given by [1]

$$\bar{\epsilon} \cdot \bar{r} = |\epsilon| \, |r| \sqrt{\frac{4}{3}\pi} \sqrt{\frac{4}{3}\pi} \sum_{\mu} Y_{1\mu}^*(\epsilon) Y_{1\mu}(\hat{r})$$

where we have expressed both vector $\vec{\epsilon}$ and $\vec{r}$ in spherical components :

$$A_\mu = |A| \sqrt{\frac{4}{3}\pi} Y_{1\mu}(\hat{A})$$

Through the dipole operator the bound state is excited in a continuum state. The wave function for a continuum electron can be written as [1]:

$$|int\rangle = \frac{1}{\sqrt{k_p}} \sum_{l_p m_p} \tilde{\Re}_{El_p}(r) Y_{l_p m_p}^*(\hat{k}) Y_{l_p m_p}^*(\hat{r}) t_{l_p} i^{l_p} X_{\sigma_p}$$

and i^{l_p} indicates the factor phase in complex field where $Y_{l_p m_p}(r)$ represents the wave function and $Y_{l_p m_p}(\hat{r})$ the spherical harmonic which describes the angular distribution and $Y_{l_p m_p}^*(\hat{k})$ is its complex conjugated; while $e^{-i\sigma_{l_p}}$ indicates always a phase factor which shifts the radial part of the matrix elements with respect to the wave function of a free electron, moreover $t_{l_p} = e^{-i\sigma_{l_p}} \sin \sigma_{l_p}$ and k_p represents the momentum of the

free electron.

Now we can write the complex conjugated of the intermediate state $\langle int|$:

$$\langle int| = \frac{1}{\sqrt{k_p}} \sum_{l_p m_p} \Re_{El_p}(\hat{r}) Y_{l_p m_p}(\hat{k}) Y^*_{l_p m_p}(\hat{r}) t^*_{l_p} i^{-l_p} X_{\sigma_p}$$

With the elements showed above it is possible to write the first step of the "Auger Effect", that is the photoemission, as:

$$\langle int |\bar{\epsilon} \cdot \bar{r}| g \rangle = \frac{1}{\sqrt{k_p}} \cdot \frac{4}{3}\pi \sum_{l_p m_p \sigma_p m_c \sigma_c \mu} \int \Re_{nl_c}(r) r \Re^*_{El_p}(r) dr$$

$$\int Y_{l_c m_c}(\hat{r}) Y^*_{l_p m_p}(\hat{r}) Y_{1\mu}(\hat{r}) \hat{d}r X_{\sigma_c} X^+_{\sigma_p} Y l_p m_p(\hat{k}) t^*_{l_p} i^{-l_p} Y^*_{1\mu}(\hat{\epsilon})$$

where $\hat{d}r = d\Omega$

$$\int Y_{l_c m_c}(\hat{r}) Y^*_{l_p m_p}(\hat{r}) Y_{1\mu}(\hat{r}) \hat{d}r = \sqrt{\frac{(2 \cdot l_c + 1)(2 \cdot 1}{+}1)4\pi(2 \cdot l_p + 1)} C^{l_p 0}_{l_c 010} C^{l_p m_p}_{l_c m_c 1\mu}$$

where $C^{l_p 0}_{l_c 010} C^{l_p m_p}_{l_c m_c 1\mu}$ represent the "Clebsch-Gordan coefficients" [1], which account for the multiplicity of each of these terms.

For the second step, we must describe the total wave function of the system as the combination of two wave functions in an anti symmetrical state, being the two particles involved described by Fermi-Dirac statistics identical. So that

$$\Psi_{Tot} = \frac{1}{2} \{\Psi(l_1(1)l_2(2)) - \Psi(l_1(2)l_2(1))\}$$

where the first part of Ψ_{Tot} is given by:

$$\Psi(l_1(1)l_2(2)) = \sum_{n_1 n_2 \sigma_1 \sigma_2} \Re_{n_1 l_1}(r_1) \Re_{n_2 l_2}(r_2) C^{LM}_{l_1 m_1 l_2 m_2} Y_{l_1 m_1}(\hat{r}_1) Y_{l_2 m_2}(\hat{r}_2) C^{SS_z}_{\frac{1}{2}\sigma_1 \frac{1}{2}\sigma_2} X_{\sigma_1}(1) X_{\sigma_2}(2)$$

where $C^{LM}_{l_1 m_1 l_2 m_2}$ represents the Clebsch-Gordon coefficient of an orbital momentum L while $C^{SS_z}_{\frac{1}{2}\sigma_1 \frac{1}{2}\sigma_2}$ represents that of the spin momentum; moreover $X_{\sigma_1}(1) X_{\sigma_2}(2)$ represent the spin states of the two electrons.

The second part of Ψ_{Tot} is given by:

$$\Psi(l_1(2)l_2(1)) = \sum_{m_1 m_2 \sigma_1 \sigma_2} \Re_{n_1 l_1}(r_2) \Re_{n_2 l_2}(r_1) C^{LM}_{l_1 m_1 l_2 m_2} Y_{l_1 m_1}(\hat{r}_2) Y_{l_2 m_2}(\hat{r}_1) C^{SS_z}_{\frac{1}{2}\sigma_1 \frac{1}{2}\sigma_2} X_{\sigma_1}(2) X_{\sigma_2}(1)$$

In this way the two quantities can be coupled and added up. By introducing the Bipolar Spherical Harmonics given by the irreducible tensorial product of spherical harmonics we obtain:

$$\sum_{m_1 m_2} C^{LM}_{l_1 m_1 l_2 m_2} Y_{l_1 m_1}(\hat{r}_1) Y_{l_2 m_2}(\hat{r}_2) \equiv \{Y_{l_1}(r_1) \otimes Y_{l_2}(r_2)\}_{LM}$$

and

$$\sum_{m_1 m_2} C^{LM}_{l_1 m_1 l_2 m_2} Y_{l_1 m_1}(\hat{r}_2) Y_{l_2 m_2}(\hat{r}_1) \equiv \{Y_{l_1}(r_2) \otimes Y_{l_2}(r_1)\}_{LM}$$

the totality of the bipolar spherical harmonics with different l_1, l_2, L e M constitute a set of functions which depend on the two vectors $\vec{r}_1$ e $\vec{r}_2$ related to the two electrons e_p^- and e_a^-.

$$
\begin{aligned}
\Psi_{Tot} =\ & \frac{1}{\sqrt{2}} \sum_{\sigma_1 \sigma_2} \Re_{n_1 l_1}(r_1) \Re_{n_2 l_2}(r_2) \{Y_{l_1}(r_1) \otimes Y_{l_2}(r_2)\}_{LM} C^{SS_z}_{\frac{1}{2}\sigma_1 \frac{1}{2}\sigma_2} X_{\sigma_1}(1) X_{\sigma_2}(2) \\
& - \frac{1}{\sqrt{2}} (-1)^{l_1+l_2-L+1-S} \Re_{n_1 l_1}(r_2) \Re_{n_2 l_2}(r_1) \{Y_{l_1}(r_2) \otimes Y_{l_2}(r_1)\}_{LM} C^{SS_z}_{\frac{1}{2}\sigma_2 \frac{1}{2}\sigma_1} \\
& X_{\sigma_1}(2) X_{\sigma_2}(1)
\end{aligned}
$$

We must now to formalize the second step of the cross section, which is the interaction of two particles caused by the coulomb interaction, but before doing this we have to define $1/r$ and $\langle f|$ as [1]:

$$\frac{1}{r} = \frac{1}{|\bar{r}_1 - \bar{r}_2|} = 4\pi \sum_{l=0}^{\infty} \frac{1}{(2l+1)} \left(\frac{r^l_<}{r^{l+1}_>}\right) \{Y_l(\Omega_2) \otimes Y_l(\Omega_1)\}_{00} \sqrt{2l+1}(-1)^{-l}$$

where $|\bar{r}_1 - \bar{r}_2|$ where $\bar{r}_1$ indicates the distance of the electron of the ion A^{++} and $\bar{r}_2$ the distance from the other electron. The expression in the brackets instead represents a tensorial product of range zero, a scalar product between the wave function $Y_l(\Omega_2)$ and $Y_l(\Omega_1)$. So we can write the final state as [1]

$$
\begin{aligned}
\langle f| =\ & \frac{1}{\sqrt{k_a}} \sum_{l_a m_a \sigma_a} \Re^*_{E l_a}(r_1) \Re_{n_c l_c}(r_2) X^+_{\sigma_a} X^+_{\sigma_c} t^*_{l_a} i^{-l_a} Y_{l_a m_a}(\hat{k}_a) \sum_M C^{L_{ac} M_{ac}}_{l_a m_a l_c m_c} \\
& \{Y_{l_a}(r_1) \otimes Y_{l_c}(r_2)\}^*_{L_{ac} M_{ac}}
\end{aligned}
$$

which represents nothing else but the product of the wave functions, one for the emitted electron and the other for the Auger electron, where $X^+_{\sigma_c}$ and $X^+_{\sigma_a}$ represent

the spin states of the two electrons.

Now that all the elements are written we can formalize the second step:

$$\left\langle f \left| \frac{e^2}{|\vec{r}_1 - \vec{r}_2|} \right| int \right\rangle = \frac{2\sqrt{2}\pi}{\sqrt{k_a}} e^2 \sum_{l=0}^{\infty} \frac{(-1)^{-l}}{\sqrt{2l+1}} \int \int \Re_{n_1 l_1}(r_1) \Re^*_{E l_a}(r_1) \frac{r^l_<}{r^{l+1}_>} \Re_{n_c l_c}(r_2)$$

$$\Re_{n_2 l_2}(r_2) dr_1 dr_2 \delta_{LL'} \delta_{MM'} \sum_{l'_1 l'_2} B^{l'_1 l'_2 l}_{l_1 l_2 l L 0} \delta_{l'_1 l_a} \delta_{l'_2 l_c} \delta_{L' L_{ac}} \delta_{M' M_{ac}} C^{SS_z}_{\frac{1}{2}\sigma_1 \frac{1}{2}\sigma_2} C^{L_{ac} M_{ac}}_{l_a m_a l_c m_c} \tag{2}$$

hence, the cross section is given by:

$$\frac{d^2\sigma}{dh_a dh_p} \propto \left| \left\langle f \left| \frac{e^2}{|\bar{r}_1 - \bar{r}_2|} \right| int \right\rangle \left\langle int \left| \bar{\epsilon} \cdot \bar{r} \right| g \right\rangle \right|^2 = \tag{3}$$

$$= \left| \frac{1}{\sqrt{k_p}} \frac{4\pi}{3} \sum_{l_p m_p m_c M} Y_{l_p m_p}(\hat{k}) t^*_{l_p} i^{-l_p} Y^*_{1\mu}(\hat{\epsilon}) \sqrt{\frac{1}{4\pi}} \sqrt{\frac{(2l_c+1)3}{(2l_p+1)}} C^{l_p 0}_{l_c 010} C^{l_p m_p}_{l_c m_c 1\mu} 2e^2 \frac{2\sqrt{2}\pi}{\sqrt{k_a}} \right.$$

$$\int \Re_{n l_c}(r) r \Re^*_{E l_p}(r) dr \int \int \Re^*_{E l_a}(r_1) \Re_{n_1 l_1}(r_1) \frac{r^l_<}{r^{l+1}_>} \Re_{n_2 l_2}(r_2) \Re_{n_c l_c}(r_2) dr_1 dr_2$$

$$\sum_{l=0}^{\infty} \frac{(-1)^{-l}}{\sqrt{2l+1}} \delta_{LL'} \delta_{MM'} \sum_{\sigma_1 \sigma_2 l_a m_a} C^{SS_z}_{\frac{1}{2}\sigma_1 \frac{1}{2}\sigma_2} C^{L_{ac} M_{ac}}_{l_a m_a l_c m_c} C^{l_a 0}_{l_1 0 l 0} C^{l_c 0}_{l_2 0 l 0} C^{SS_z}_{\frac{1}{2}\sigma_1 \frac{1}{2}\sigma_2}$$

$$\sqrt{\frac{(2l_1+1)(2l_2+1)(2l+1)(2l+1)(2L+1)}{(4\pi)^2}} Y_{l_a m_a}(k_a) t^*_{l_a}$$

$$\left. \left\{ \begin{matrix} l_1 & l & l_a \\ l_2 & l & l_c \\ L & 0 & L \end{matrix} \right\} \right|^2$$

where Y_{xx} describe the angular dependence, and the second line defines radial matrix elements.

In the cross section expression (3) is possible to distinguish the radial matrix elements and the spherical harmonic as $Y_{l_p m_p}(k_p)$, $Y^*_{1\mu}(\epsilon)$, $Y_{l_a m_a}(k_a)$; that describe the kinematic, of the process.

We can plot the result of the calculations varying the direction of the light polarization and the direction of electrons.

Then the calculations have been performed for the Xenon atom, and the transition we

8

considered is the one in with a core hole created in the $4d$ level and the final holes both in the $5p$ level.

We can synthesize the Xenon figures, with table 1, in which we describe the kinematical condition under which cross section have been computed.

Without Xenon the radial matrix elements	θ_p	ϕ_p	θ_a	ϕ_a
figure 2	$\frac{\pi}{2}$	0	$\frac{\pi}{2}$	variable
figure 3	$\frac{\pi}{2}$	$\frac{5\pi}{6}$	$\frac{\pi}{2}$	variable
figure 4	$\frac{\pi}{2}$	variable	$\frac{\pi}{2}$	0
figure 5	$\frac{\pi}{2}$	variable	$\frac{\pi}{2}$	$\frac{5\pi}{6}$
With Xenon the radial matrix elements	θ_p	ϕ_p	θ_a	ϕ_a
figure 6	$\frac{\pi}{2}$	0	$\frac{\pi}{2}$	variable
figure 7	$\frac{\pi}{2}$	$\frac{5\pi}{6}$	$\frac{\pi}{2}$	variable
figure 8	$\frac{\pi}{2}$	variable	$\frac{\pi}{2}$	0
figure 9	$\frac{\pi}{2}$	variable	$\frac{\pi}{2}$	$\frac{5\pi}{6}$
Experimental date from literature	θ_p	ϕ_p	θ_a	ϕ_a
figure 10	$\frac{\pi}{2}$	$\frac{5\pi}{6}$	$\frac{\pi}{2}$	variable
Calculation from literature "multi-electron method"	θ_p	ϕ_p	θ_a	ϕ_a
figure 11	$\frac{\pi}{2}$	$\frac{5\pi}{6}$	$\frac{\pi}{2}$	variable

Table 1: Summery of conditions upon which the Auger-photoelectron angular correlation has been calculated with the light linearly polarized.

In the fig 2 the angle ϕ_p of the photoelectron has been set along the polarization ($\theta_p = \frac{\pi}{2}$ and $\phi_p = 0$) and the Auger scanning takes place in the plane perpendicular to

the beam direction with ($\theta_a = \frac{\pi}{2}$ and ϕ_a variable). We can observe that there are four lobes, and they have an symmetry axis that correspond with photoelectron direction and polarization light angle at $\theta_p = \frac{\pi}{2}$ and $\phi_p = 2\pi + k\pi$ and an symmetry axis that correspond at $\theta_p = \frac{\pi}{2}$ and $\phi_p = \frac{\pi}{2} + k\pi$. Moreover this figure has a node in intersection point of the axis patterns.

In the fig 3 we detect the photoelectron at $\theta_p = \frac{\pi}{2}$ $\phi_p = \frac{5\pi}{6}$ and $\theta_p = \frac{\pi}{2}$ and then the
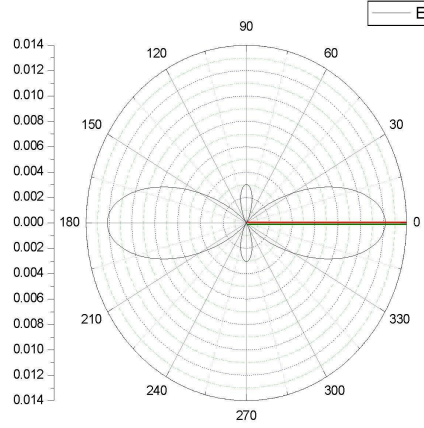
Figure 2: *Plot of the cross section of Auger effect when photo-electron e_p^- is detected at $\theta_p = \frac{\pi}{2}$ and $\phi_p = 0$ and with $\theta_a = \frac{\pi}{2}$ and ϕ_a variable with the light linearly polarized (line red is photoelectron, line green is polarization light).*

Auger electron is scanned in the plane perpendicular to the photon bean with $\theta_a = \frac{\pi}{2}$ and ϕ_a variable. We can observe that there are four lobes, and they have two symmetry axis: $\theta_p = \frac{\pi}{2}$, $\phi_p = \frac{\pi}{6} + k\pi$ and $\theta_p = \frac{\pi}{2}$, $\phi_p = \frac{2\pi}{3} + k\pi$,. This figure has a node in the intersection point of the axis patterns.

The same identical procedure has been followed in the case where once the Auger position is set $\theta_a = \frac{\pi}{2}$ and $\phi_a = 0$ and the photoelectron is placed in the perpendicular plane at $\theta_p = \frac{\pi}{2}$ and ϕ_p variable in the fig 4. In this figure we can see six lobes, there are three symmetry axis: the first at $\theta_a = \frac{\pi}{2}$, $\phi_a = 2\pi + k\pi$; the second at $\theta_a = \frac{\pi}{2}$, $\phi_a = \frac{\pi}{3} + k\pi$; and the last at $\theta_a = \frac{\pi}{2}$, $\phi_a = \frac{2\pi}{3} + k\pi$. Moreover there is a node in the intersection point of the axis patterns.
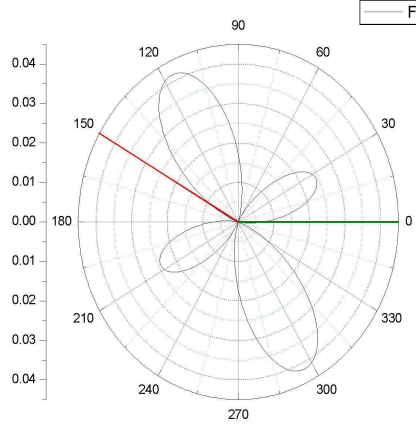
Figure 3: *Plot of the cross section of Auger effect when photo-electron e_p^- and is detected at $\theta_p = \frac{\pi}{2}$ and $\phi_p = \frac{5\pi}{6}$ and with $\theta_a = \frac{\pi}{2}$ and ϕ_a variable and with the light linearly polarized (line red is photoelectron, line green is polarization light).*

The fig 5 shows instead the case in which the Auger scanning is set at $\theta_a = \frac{\pi}{2}$ and at $\phi_a = \frac{5\pi}{6}$ and the photoelectron it is detected in the plane perpendicular with $\theta_p = \frac{\pi}{2}$ and ϕ_p variable. In this figure we can see six lobes, there are three symmetry axis: the first at $\theta_a = \frac{\pi}{2}$, $\phi_a = \frac{\pi}{3} + k\pi$; the second at $\theta_a = \frac{\pi}{2}$, $\phi_a = \frac{11\pi}{18} + k\pi$; and the last at $\theta_a = \frac{\pi}{2}$, $\phi_a = \frac{5\pi}{6}$. Moreover there is a node in the intersection point of the axis patterns. In the fig 6 we study the photoelectron at $\theta_p = \frac{\pi}{2}$ and $\phi_p = 0$, with the Auger emission direction in the plane perpendicular to the direction of the beam with $\theta_a = \frac{\pi}{2}$ and ϕ_a variable. We can observe that there are four lobes, and they have two symmetry axis: the first at $\theta_p = \frac{\pi}{2}$, $\phi_p = 0$, ; the second at $\theta_p = \frac{\pi}{2}$, $\phi_p = \frac{\pi}{2}$. This figure has a node in the intersection point of the axis patterns. However this is not dearly visible in the angular plot, since the anisotropy is still very hight.

In the fig 7 we study the photoelectron at $\theta_p = \frac{\pi}{2}$ and $\phi_p = \frac{5\pi}{6}$, with the Auger emission direction in the plane perpendicular to the direction of the beam with $\theta_a = \frac{\pi}{2}$ and ϕ_a variable, including the radial matrix elements. We can observe that there is a lobe, and it has two symmetry axis at $\theta_p = \frac{\pi}{2}$, $\phi_p = \frac{11\pi}{12} + k\pi$ and at $\theta_p = \frac{\pi}{2}$, $\phi_p = \frac{5\pi}{12} + k\pi$ that doesn't correspond with photoelectron direction and polarization light. Moreover this

11
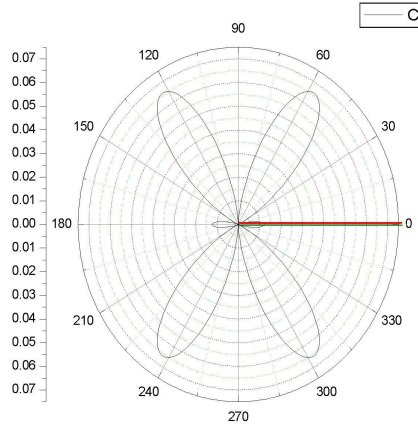
Figure 4: *Plot of the cross section of Auger effect when the Auger position is given by* e_a^- *and* $\theta_a = \frac{\pi}{2}$, $\phi_a = 0$ *and with* $\theta_p = \frac{\pi}{2}$ *and* ϕ_p *variable and with the light linearly polarized (line red is Auger electron, line green is polarization light).*
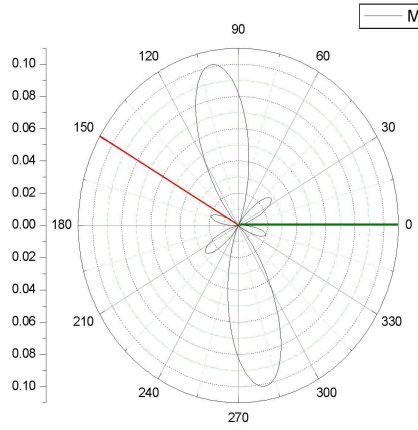
Figure 5: *Plot of the cross section of Auger effect when the Auger position is given by* $\theta_a = \frac{\pi}{2}$, $\phi_a = \frac{5\pi}{6}$ *and with* $\theta_p = 90^o$ *and* ϕ_p *variable and with the light linearly polarized (line red is Auger electron, line green is polarization light).*
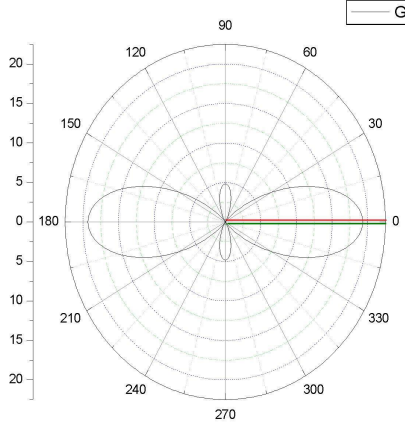
Figure 6: *Plot of the cross section of Auger effect when photo-electron e_p^- is detected at $\theta_p = \frac{\pi}{2}$ and $\phi_p = 0$ and with $\theta_a = \frac{\pi}{2}$ and ϕ_a variable with the light linearly polarized (line red is photoelectron, line green is polarization light) including the radial matrix elements.*

figure has a relative minimum at $\theta_p = \frac{\pi}{2}$ and $\phi_p = \frac{\pi}{4} + k\pi$ and an absolute minimum at $\theta_p = \frac{\pi}{2}$ and $\phi_p = \frac{11\pi}{18} + k\pi$.

Now we can analyze the fig 8 in which once the Auger direction of emission is set at $\theta_a = \frac{\pi}{2}$ and $\phi_a = 0$ and the photoelectron is detected in the perpendicular plane with $\theta_p = \frac{\pi}{2}$ and ϕ_p variable. We can observe that there is a lobe, and it has symmetry axis that corresponds with Auger direction and polarization light $\theta_a = \frac{\pi}{2}$, $\phi_a = 2\pi + k\pi$. This figure has an absolute minimum at $\theta_a = \frac{\pi}{2}$, $\phi_a = \frac{\pi}{2}$.

Now we can analyze the fig 9 in which once the Auger direction of emission is set at $\theta_a = \frac{\pi}{2}$ and $\phi_a = \frac{5\pi}{6}$ and the photoelectron is detected in the perpendicular plane with $\theta_p = \frac{\pi}{2}$ and ϕ_p variable. We can observe that it has a lobe, and it has two symmetry axis: the first at $\theta_a = \frac{\pi}{2}$, $\phi_a = \frac{11\pi}{18} + k\pi$ and at $\theta_a = \frac{\pi}{2}$, $\phi_a = \frac{\pi}{4} + k\pi$. This figure has a relative minimum at $\theta_a = \frac{\pi}{2}$, $\phi_a = \frac{\pi}{9}$ and an absolute minimum at $\theta_a = \frac{\pi}{2}$ and $\phi_p = \frac{\pi}{3}$.

Now by introducing the theoretical data, fig 10, is possible to understand if the used model reflects the experiment. Moreover we can compare the results of the calculations

13
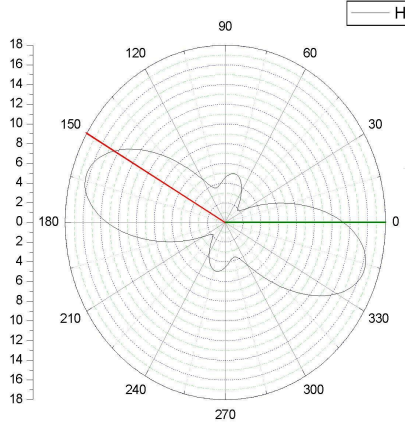
Figure 7: *Plot of the cross section of Auger effect when photo-electron* e_p^- *is detected at* $\theta_p = \frac{\pi}{2}$ *and* $\phi_p = \frac{5\pi}{6}$ *and with* $\theta_a = \frac{\pi}{2}$ *and* ϕ_a *variable with the light linearly polarized (line red is photoelectron, line green is polarization light) including the radial matrix elements.*
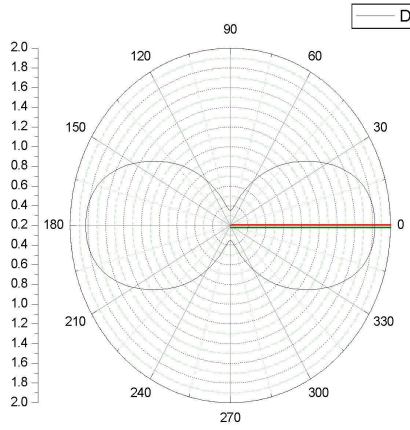
Figure 8: *Plot of the cross section of Auger effect when the Auger position is given by* e_a^- *and* $\theta_a = \frac{\pi}{2}$, $\phi_a = 0$ *and with* $\theta_p = \frac{\pi}{2}$ *and* ϕ_p *variable and with the light linearly polarized (line red is Auger electron, line green is polarization light) including the radial matrix elements.*

14
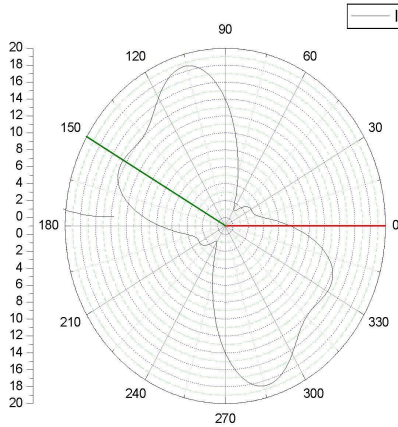
Figure 9: *Plot of the cross section of Auger effect when the Auger position is given by e_a^- and $\theta_a = \frac{\pi}{2}$, $\phi_a = \frac{5\pi}{6}$ and with $\theta_p = \frac{\pi}{2}$ and ϕ_p variable and with light linearly polarized (line red is Auger electron, line green is polarization light) including the radial matrix elements.*

with the experimental data existing in literature [4] fig 11, where calculation is performed within a relativistic many body model i.e , the wave functions of all electrons are taken into account, and the relativistic effects too.

In experimental data in literature, fig 11, we can observe that the theoretical model developed in this thesis individuates the rise of the lobe but overestimates the intensity of the lobes and only two points in the experimental data are near the theoretical curve; instead in the theoretical model of the literature data [4], we can see that the symmetry of the picture does not coincide neither with the direction of the polarized light nor with the direction of the Auger direction $\theta_a = \frac{\pi}{2}$, $\phi_a = \frac{5\pi}{6}$ but it reflects faithfully the experimental data.

Then the calculations have been performed on Magnesium atom, and the transition we considered is the one in which a core hole is created in the $2p$ level and the final holes are both in a $3s$ level.

It is possible now to show as the model elaborated in this thesis, using an atom as
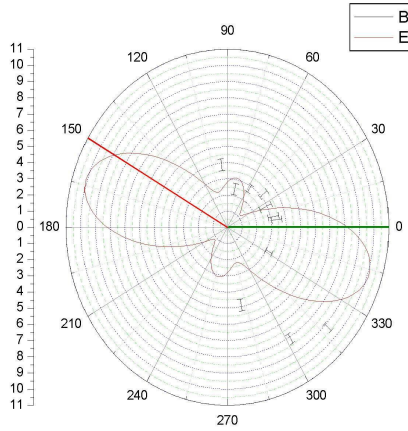
Figure 10: *Plot of the cross section of Auger effect when photo-electron* e_p^- *is detected at* $\theta_p = \frac{\pi}{2}$ *and* $\phi_p = \frac{5\pi}{6}$ *and with* $\theta_a = \frac{\pi}{2}$ *and* ϕ_a *variable with the light linearly polarized (line red is photoelectron, line green is polarization light) including the radial matrix elements and the experimental data.*
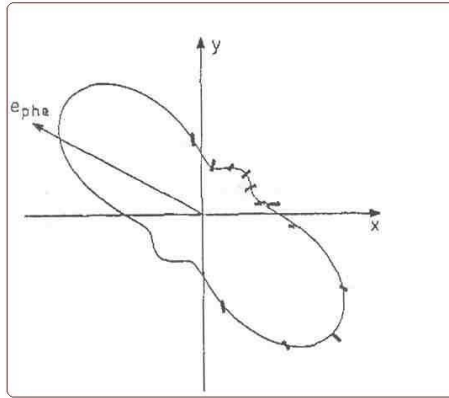
Figure 11: *Plot of the cross section of Auger effect in literature [4] when photo-electron* e_p^- *is detected at* $\theta_p = \frac{\pi}{2}$ *and* $\phi_p = \frac{5\pi}{6}$ *and with* $\theta_a = \frac{\pi}{2}$ *and* ϕ_a *variable with the light linearly polarized inserting the radial matrix elements, including the experimental data.*

Excluding the radial matrix elements	θ_p	ϕ_p	θ_a	ϕ_a
figure 12	$\frac{\pi}{2}$	variable	$\frac{\pi}{2}$	0
figure 13	$\frac{\pi}{2}$	variable	$\frac{\pi}{2}$	$\frac{5\pi}{6}$
Including the radial matrix elements	θ_p	ϕ_p	θ_a	ϕ_a
figure 14	$\frac{\pi}{2}$	variable	$\frac{\pi}{2}$	$\frac{5\pi}{6}$
Experimental date from literature	θ_p	ϕ_p	θ_a	ϕ_a
figure 15	$\frac{\pi}{2}$	variable	$\frac{\pi}{2}$	$\frac{5\pi}{6}$

Table 2: Summery of conditions upon which the Auger-photoelectron angular correlation has been calculated with the light linearly polarized.

the Magnesium, gives better results. This is due to the fact that the Magnesium is a lighter atom than Xenon and so "'relativistic effects"' and "'many electrons"' are less relevant.As a matter of fact we can see in fig 12, in which once the Auger direction of emission is set at $\theta_a = \frac{\pi}{2}$ and $\phi_a = 0$ and the photoelectron is detected in the perpendicular plane with $\theta_p = \frac{\pi}{2}$ and ϕ_p variable. We can observe that there is a lobe, and it has symmetry axis that corresponds with Auger direction and polarization light $\phi_a = 0$. We can observe that there are two lobes, and they have two symmetry axis: the first at $\theta_a = \frac{\pi}{2}$, $\phi_a = 0$ and the second at $\theta_a = \frac{\pi}{2}$, $\phi_a = \frac{\pi}{2} + k\pi$. This figure has a node in the intersection point of the axis patterns.

In the fig 13 in which once the Auger direction of emission is set at $\theta_a = \frac{\pi}{2}$ and $\phi_a = \frac{5\pi}{6}$ and the photoelectron is detected in the perpendicular plane with $\theta_p = \frac{\pi}{2}$ and ϕ_p variable. We can observe that there two lobes, and they have two symmetry axis: the first at $\theta_a = \frac{\pi}{2}$, $\phi_a = \frac{11\pi}{18} + k\pi$ and the second at $\theta_a = \frac{\pi}{2}$, $\phi_a = 2\pi + k\pi$. This figure has a node in the intersection point of the axis patterns.

In the end, we can analyze the fig 14, in which once the Auger direction of emission
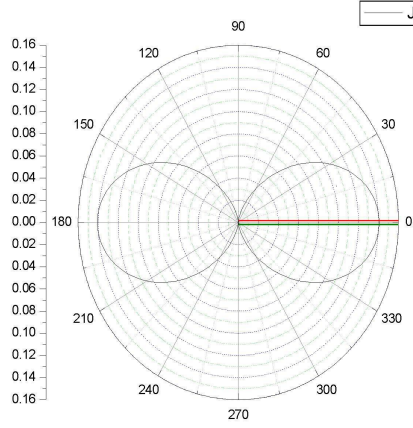
Figure 12: *Plot of the cross section of Auger effect when the Auger position is given by e_a^- and $\theta_a = \frac{\pi}{2}$, $\phi_a = 0$ and with $\theta_p = \frac{\pi}{2}$ and ϕ_p variable and with light linearly polarized (line red is Auger electron, line green is polarization light), excluding the radial matrix elements.*
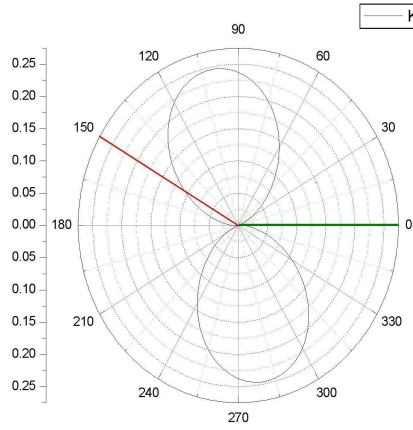
Figure 13: *Plot of the cross section of Auger effect when the Auger position is given by e_a^- and $\theta_a = \frac{\pi}{2}$, $\phi_a = \frac{5\pi}{6}$ and with $\theta_p = \frac{\pi}{2}$ and ϕ_p variable and with light linearly polarized (line red is Auger electron, line green is polarization light) including the radial matrix elements.*

is set at $\theta_a = \frac{\pi}{2}$ and $\phi_a = 0$ and the photoelectron is detected in the perpendicular plane with $\theta_p = \frac{\pi}{2}$ and ϕ_p variable. We can observe that there is a lobe, and there are two symmetry axis: the first at $\theta_p = \frac{\pi}{2}$, $\phi_a = \frac{3\pi}{4} + k\pi$ and the second at $\theta_p = \frac{\pi}{2}$, $\phi_a = \frac{\pi}{4} + k\pi$. Moreover there is a node in the intersection point of the axis patters.

We can analyze the fig 15 in which once the Auger direction of emission is set at
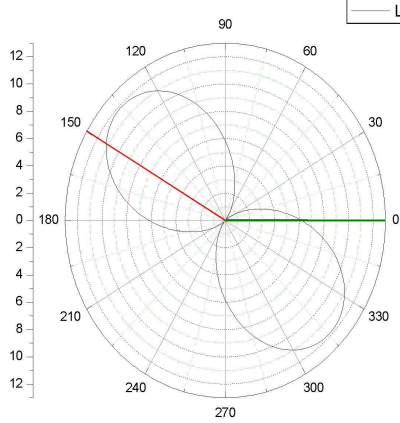
Figure 14: *Plot of the cross section of Auger effect when the Auger position is given by e_a^- and $\theta_a = 90^o$, $\phi_a = 150^o$ and with $\theta_p = 90^o$ and ϕ_p variable and with light linearly polarized (line red is Auger electron, line green is polarization light) excluding the radial matrix elements.*

$\theta_a = 0$ and $\phi_a = \frac{5\pi}{6}$ and the photoelectron is detected in the perpendicular plane with $\theta_p = \frac{\pi}{2}$ and ϕ_p variable. We can observe a lobe, there are two symmetry axis: the first at $\theta_a = \frac{\pi}{2}$ $\phi_a = \frac{11\pi}{12} + k\pi$ and the second at $\theta_a = \frac{\pi}{2}$, $\phi_a = \frac{\pi}{4}$. Moreover there is a minimum in $\theta_a = \frac{\pi}{4} + k\pi$ and $\phi_a = \frac{\pi}{2}$.

We can conclude this study saying that: the model developed in this thesis within the frame of closed shell atoms and single particle approach, does not involve all the electrons but only those that are strictly involved in the transition. Moreover the relativistic effects are excluded in our simple model: the radial parts through which the matrix elements have been calculated are considered to be solutions of a Schroedinger
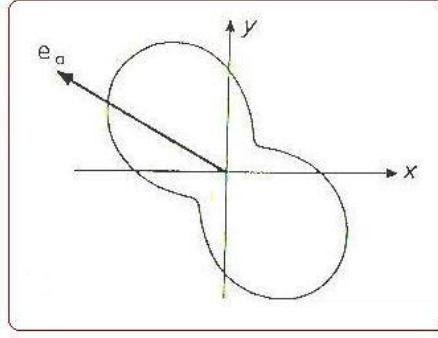
Figure 15: *Plot of the cross section of Auger effect in literature [3] when the Auger position is given by e_a^- and $\theta_a = \frac{\pi}{2}$, $\phi_a = \frac{5\pi}{6}$ and with $\theta_p = \frac{\pi}{2}$ and ϕ_p variable and with light linearly polarized (line red is Auger electron, line green is polarization light) including the radial matrix elements.*

equation which is not relativistic.

Our model is good in atoms with few electrons but have serious problems in more complex atoms because it doesn't consider all wave functions of electrons and relativistic effects that are very important in a heavy atom.

The future developments of this method will be to consider wave function of the last level and relativistic effects. We have developed a simple model because it use less wave functions and it is described in a specific analytic representation. This model is right for a light atom because the most important characteristics are produced in a good form. With corrective factors this model could describe heavy atoms and so we will have a simple model to calculate the heavy atoms cross section.

References

[1] Chattarjy, D. *The Theory of Auger Transition* Academic Press, San Diago, CA, 1976

[2] T.A.Carlson *Photo-electron and Auger Spectroscopy* Plenum Press, New York,

1975

[3] D.R.Hartree *The calculation of atomic structure* New York: Wiley, 1957

[4] T.Koopmans *Physica 1* 104-113 1934